APPLIED PHYSICS

Light-induced assembly of living bacteria with honeycomb substrate

Shiho Tokonami[1,2]*, Shinya Kurita[1,2], Ryo Yoshikawa[1,2], Kenji Sakurai[1,2], Taichi Suehiro[1,2,3], Yasuyuki Yamamoto[1,2,3], Mamoru Tamura[2,3], Olaf Karthaus[4], Takuya Iida[2,3]*

Some bacteria are recognized to produce useful substances and electric currents, offering a promising solution to environmental and energy problems. However, applications of high-performance microbial devices require a method to accumulate living bacteria into a higher-density condition in larger substrates. Here, we propose a method for the high-density assembly of bacteria (10^6 to 10^7 cells/cm^2) with a high survival rate of 80 to 90% using laser-induced convection onto a self-organized honeycomb-like photothermal film. Furthermore, the electricity-producing bacteria can be optically assembled, and the electrical current can be increased by one to two orders of magnitude simply by increasing the number of laser irradiations. This concept can facilitate the development of high-density microbial energy conversion devices and provide new platforms for unconventional environmental technology.

INTRODUCTION

The broad application potential of a wide variety of beneficial bacteria is increasingly recognized by exploiting bacterial metabolic mechanisms, including the purification of useful organic compounds for sewage treatment and bioethanol production (*1*) and acquisition of electrical energy (*2*). In addition to basic evaluations of the metabolic mechanisms of these target bacteria, their high-density assembly on a substrate in a viable state is an essential requirement for applications of beneficial bacteria with high efficiency (*3*). The type of bacteria selected depends on the application, with the genera *Geobacter* and *Shewanella* being the most common sources of electricity-producing bacteria. These primitive bacteria are known to emit electrons derived from the oxidation-reduction reaction occurring inside the cells while retaining abundant energy for other processes (*4*, *5*). The cytochromes in the metabolic organelles of many bacteria are water insoluble, whereas cytochrome c is a water-soluble protein on the surface of electricity-producing bacteria, which mediates the generation of electrons during decomposition using organic matter as an energy source. Because electrons can be efficiently emitted outside the cell via this metabolic mechanism, the application of these electricity-producing bacteria to microbial fuel cells is expected (*6*). Toward this end, substantial research effort has focused on improving the efficiency of electron acquisition by exploiting this electron transfer mechanism by bringing electricity-producing bacteria into contact with electrodes with large surface areas such as porous carbon and graphene nanoribbons (*7*, *8*). These bacteria range in size from several hundred nanometers to several micrometers. However, using a substrate with pores of about 1 to 10 μm diameter that are closely arranged could maximize the contact area to accommodate a larger number of bacteria to increase the efficiency of the system. In particular, the electricity production can be maximized by trapping the bacteria alive. From this point of view, a substrate with a honeycomb structure, comprising closely packed hexagonal forms, has particularly attractive features for trapping bacteria. The honeycomb represents a ubiquitous structure with the highest density found in nature (*9*–*11*), with prime examples of the macroscopic honeycomb structure as a unit that can accommodate abundant nectar with only a small amount of material, insect compound eyes that increase the surface area and sensitive detection of photons, and turtle shells that disperse stress from various directions to protect the body. Moreover, a honeycomb structure is found in organs that require a great volume and strength per area (*12*–*15*) and has been applied for bioinspired technologies (*16*, *17*).

Here, we propose a principle for the rapid and high-density trapping of a large number of bacteria in a physical manner using our developed honeycomb polymer film with pores suitable for micrometer-order bacteria in conjunction with an external field. For this purpose, it is first necessary to clarify the physicochemical mechanism to attract bacteria to the periodic honeycomb pores. As a material for the honeycomb polymer film, a matrix polymer and an amphiphilic polymer can be used in combination with water droplet self-organization (*10*). In particular, a honeycomb substrate made of polystyrene as a polymer film was used because it is not harmful to biological cells. However, because a honeycomb structure of nanometer to micrometer dimensions is highly water repellent, it is necessary to generate an external force to overcome this repellency and enable the accumulation of bacterial cells in the pores. Many bacteria have flagella with a chemotaxis function origin, which allows them to move independently according to chemical concentration gradients and other stimuli. Therefore, it is a challenge to simultaneously increase the density of target bacteria while immobilizing them onto a substrate without losing viability or the metabolic mechanism. Conventional methods of bacterial fixation include those based on electrostatic interactions and use of a binder substance such as aminothiol on the electrode substrate (*18*). However, these methods depend on the surface features of the bacteria and the length of the binder molecules and are associated with many problems such as inhibiting the electron transfer between the cells and the substrate. Therefore, it is necessary to develop a technique for trapping the bacterial cells at high density while maintaining the metabolic mechanism without using a binder substance.

[1]Department of Applied Chemistry, Graduate School of Engineering, Osaka Prefecture University, Sakai 599-8570, Japan. [2]Research Institute for Light-induced Acceleration System, Osaka Prefecture University, Sakai 599-8570, Japan. [3]Department of Physical Science, Graduate School of Science, Osaka Prefecture University, Sakai, Osaka 599-8570, Japan. [4]Department of Applied Chemistry and Bioscience, Chitose Institute of Science and Technology, Chitose, Hokkaido 066-8655, Japan.
*Corresponding author. Email: t-iida@p.s.osakafu-u.ac.jp (T.I.); tokonami@chem.osakafu-u.ac.jp (S.T.)

One potential physical method to achieve this goal is to use dielectrophoresis for collecting bacteria via an alternating electric field. However, this requires a suitable process of preparing a microelectrode, and even if the bacteria can effectively be trapped on the electrode, it is still difficult to increase the density of bacteria at the target region (*19*, *20*). Optical tweezers that use an electromagnetic light-induced force (also called photon pressure) can trap a few cells nonthermally without exerting damage but are not suitable for large-area and high-density assembly (*21*, *22*). As an alternative, the use of the convection from the photothermal effect could allow the control of the movement of the nanomaterials and micromaterials without contact over a wide spatial range on the order of submillimeters (*23*–*25*). With this approach, biochemical reactions such as molecular recognition can be exploited without losing biological functions (*26*). In particular, the bacteria can be assembled on a flat gold nanofilm by thermal convection, and the microbubbles generated by laser irradiation along with the total number of bacterial cells in the dispersion could be measured in only a few minutes, which is very rapid in comparison with the conventional culture method requiring 24 to 48 hours (*27*–*29*). Therefore, the target objects can be assembled in the vicinity of the irradiation point using thermal convection in a liquid that is locally heated by the electron-lattice interaction in the metallic thin film induced by laser irradiation. However, because most of the bacteria will be killed by the photothermal effect due to the efficient heat transfer in a flat metallic film, the survival rate will be prohibitively low.

To overcome such a trilemma of simultaneously achieving a high substrate area, high bacterial density, and good survival, we developed a honeycomb substrate for light-induced assembly (HS-LIA) using a self-organization approach. Specifically, the substrate was designed on the basis of electromagnetic and thermodynamic properties as an unconventional trapping method of bacteria under light-induced convection generated by laser irradiation (Fig. 1 and fig. S1), and the function of the trapped bacteria was electrochemically evaluated to determine the feasibility in practical application.

RESULTS

Preparation of the honeycomb polymer film

A light-absorbing thin film was formed on the surface of the honeycomb polymer (see Methods) and observed under an optical microscope (Fig. 2A and fig. S2B). Specifically, water droplets were arranged in a hexagonal closely packed manner on the surface of the polymer solution, which subsequently evaporated to form a polymer film in which the honeycomb-shaped pores are periodically arranged (fig. S2A). Subsequently, gold coating was performed with an ion-sputtering apparatus to form a gold thin film of about 50 nm. Thus, a structure was formed comprising approximately circular pores with a diameter of about 5 μm arranged in a hexagonal lattice pattern. Scanning electron microscopy showed that the depth of each pore was about 3 μm (fig. S2C). Furthermore, the cross-sectional images of pores showed that a small hole was present in the partition wall between a pair of pores as a remnant of water droplets in the self-organization process. Elemental analysis using energy-dispersive x-ray spectrometry (fig. S3) indicated that the carbon was derived from the polystyrene and polyion complex, silicon was contained in the glass substrate, and gold was derived from the thin film coated on the surface of the substrate to achieve the photothermal effect.

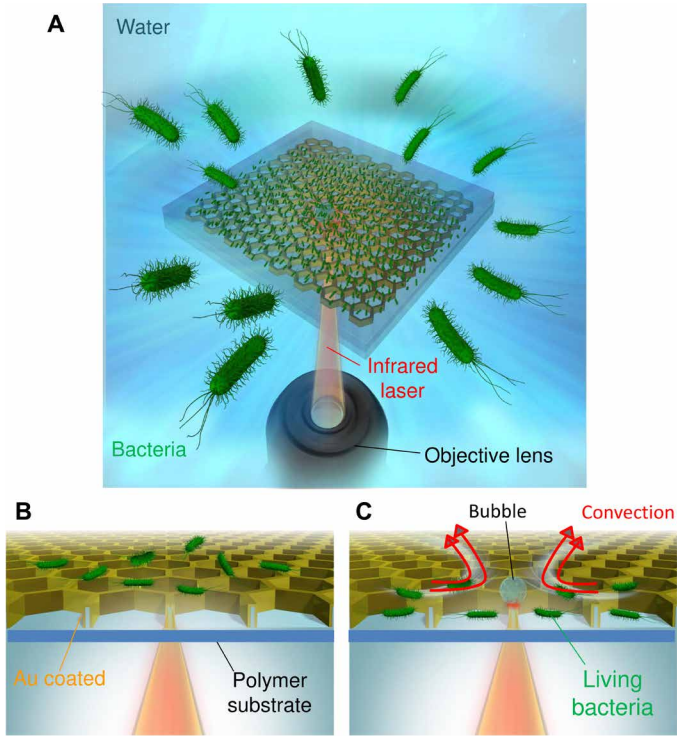

Fig. 1. Bacteria trapped by a honeycomb light–guided substrate. (**A**) Conceptual diagram of the LIA of bacteria with a large area, high density, and high survival rate by laser-induced convection. (**B**) Schematic diagram of the initial process of LIA. (**C**) Schematic diagram of convection after bubble generation and trapping of bacteria in the pores on the honeycomb substrate.

Trapping bacteria with laser irradiation

Next, we used HS-LIA to effectively trap bacteria on the substrate by laser irradiation in Fig. 2 (B to E) with the optical setup of fig. S1. For this evaluation, we used *Pseudomonas aeruginosa* as a representative Gram-negative bacterium and *Staphylococcus aureus* as representative Gram-positive bacterium. Figure 2 (B and C) shows the fluorescence images of live bacteria (green) and bacteria with a damaged outer membrane (red) when photothermal assembly was performed on the partition walls of the honeycomb polymer film using a laser power of 40 mW (see also movie S1). The survival rate was maintained at high levels of around 80 to 90% over a wide range of laser power. Moreover, bacteria were living in each pore even after laser irradiation (fig. S5 and movie S2) and growth was confirmed when the bacteria were dispersed and cultured even after laser irradiation (fig. S5). Furthermore, the relationship between laser power (which was raised from 10 mW to 70 mW) and the survival rate was evaluated based on the fluorescence images. From 30 mW to 50 mW, the bacteria densely accumulated in the honeycomb polymer film over a wide spatial range of 100 μm for both *P. aeruginosa* and *S. aureus* (figs. S6 and S7). At a lower laser power with small bubbles formed, the bacteria were more concentrated in the center and were effectively trapped in the honeycomb pores. By contrast, large bubbles were generated in the central region due to strong local heat generation with a laser power higher than 50 mW, which would be an obstacle for the accumulation of bacteria in the center of the film.

Optimization of LIA

To investigate the best method for the highly efficient LIA by HS-LIA, we also conducted a comparative experiment using a flat gold thin

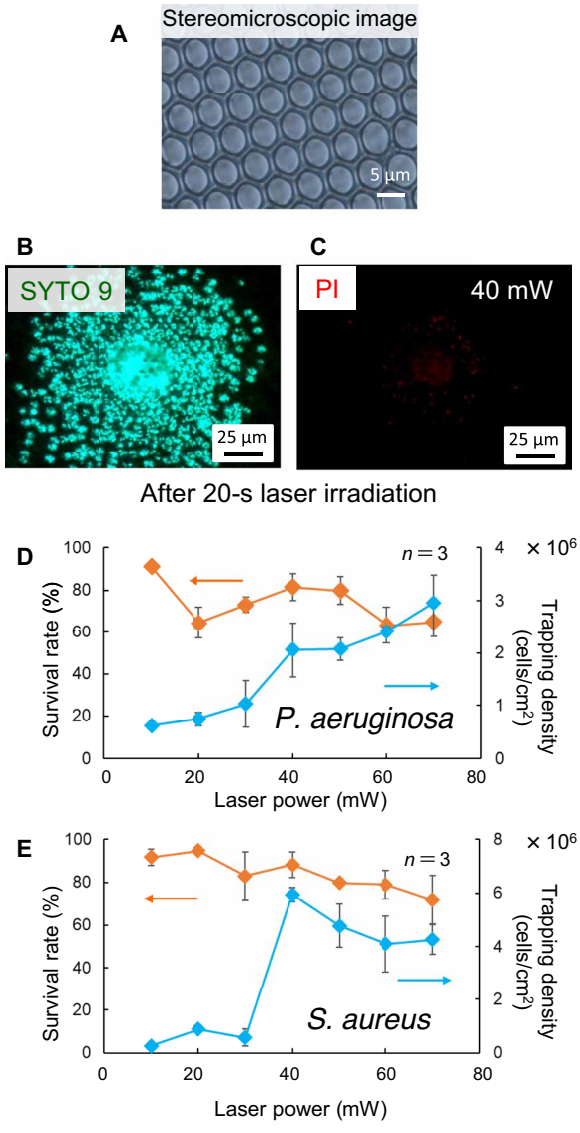

Fig. 2. Fluorescence image and survival rate of high-density LIA on the honeycomb substrate. (**A**) Stereomicroscopic image of the honeycomb substrate. (**B**) Fluorescence image (SYTO 9 staining; green) in a mixed state of live and dead bacteria. (**C**) Fluorescence image of dead bacteria [propidium iodide (PI) staining; red]. (**D**) Laser power dependence of *P. aeruginosa* trapping density and survival rate. (**E**) Laser power dependence of *S. aureus* capture density and survival rate.

film of 10-nm thickness without the honeycomb structure reported previously (*27*, *28*). As shown in fig. S8, a laser power higher than 100 mW was required to obtain a sufficiently high local temperature (close to 100°C) to generate water vapor bubbles. However, using the flat gold film of 50-nm thickness, which is the same as that coated on HS-LIA in this study, the temperature only increased by 1.3°C from the initial room temperature even with 350-mW laser irradiation, and bacteria cannot be assembled without bubble generation under the laser power range from 10 mW to 70 mW used in Fig. 2 and even under several hundreds milliwatts. Because the reflectance of the 50-nm gold thin film is considered to be the same for both the flat gold film and HS-LIA, the observed difference is likely attributed to the differences in the thermal properties of the flat substrate and HS-LIA. The thermal conductivity of the 50-nm gold film is about 200 W/(m·K) [100 W/(m·K) for a 10-nm-thick film and 320 W/(m·K) for bulk gold] (*30*), whereas the thermal conductivity of polystyrene, as the material of the honeycomb polymer film, is 0.1 W/(m·K), that of the underlying glass is 1.0 W/(m·K), and that of water as a dispersion medium is 0.6 W/(m·K). Thus, although the gold thin film on the surface of the partition wall in the pores of the honeycomb substrate has the same thickness of 50 nm, the relatively low thermal conductivity of polystyrene could accumulate the heat under the laser focusing at the top and sides of the wall, as shown in Fig. 1B. In the case of the flat gold film, the heat from the laser would be rapidly dissipated from the laser irradiation point because of the high thermal conductivities of the gold film and glass substrate. These complex factors would contribute to the concentrated heating for the efficient generation of light-induced convection and microbubbles, as shown in Fig. 1C. Moreover, the scanning electron microscopy image in fig. S2C showed that the pores are interconnected, and this structure further improved horizontal "water drainage," which, in turn, contributed to the improved trapping efficiency of bacteria. As shown in Fig. 2D, the capture density of *P. aeruginosa* increased to 3×10^6 cells/cm^2 at 70 mW with increasing laser power. However, as shown in Fig. 2E, *S. aureus* showed the maximum capture density of 6×10^6 cells/cm^2 at 40 mW. The initial concentrations of *P. aeruginosa* and *S. aureus* were 9.67×10^8 colony-forming units (CFU)/ml and 1.74×10^8 CFU/ml, respectively; thus, although the concentration of *P. aeruginosa* was 5.6 times higher than that of *S. aureus*, the relation was reversed after LIA, with *S. aureus* doubling in relation to *P. aeruginosa*. This difference can be attributed to the chemotaxis of *P. aeruginosa* with flagella, whereas *S. aureus* without chemotaxis is more readily trapped. For both species, the number of trapped bacteria was considerably small at a laser power lower than 30 mW, because the light-induced convection was too weak to effectively transport the bacteria. At 40 mW, there was a peak in the number of trapped bacteria; however, the formation of large bubbles prevented the trapping of bacteria, as mentioned above.

Optimizing bacterial survival at high density

Figure 2 (D and E) shows the number of green and red luminescent spots of bacteria stained with SYTO 9 (all live and dead bacteria are stained green) and propidium iodide (PI) (only dead bacteria with a damaged outer membrane are stained red). The survival rate calculated from the number of these green and red bright points (see the "LIA of bacteria" in Methods) reached up to 80 to 90% with a laser power between 30 mW to 50 mW along with high-density assembly under certain conditions. As shown in Fig. 2C, the outer cell membrane showed evident damage due to local heat generation. Bacterial viability at each laser power was higher than 60% for *S. aureus*, whereas variations in laser power had a greater effect on the viability of *P. aeruginosa*. This is considered to also be related to the chemotaxis of the bacteria as described above. The survival rate of *P. aeruginosa* assembled by convection was estimated to be lower in the low-power region because the living cells were able to escape from the observation region before becoming trapped in the pores. As a comparative experiment, using a flat gold thin film (10 nm), at 74 mW, which is close to the maximum laser power on the honeycomb substrate, no light-induced bubble was generated, although this gentle light-induced convection could not assemble bacteria (fig. S8). However, with laser power higher than 129 mW, light-induced bubbles were generated and the bacteria assembled around this bubble, but the survival rate

was only about 15.8% for *P. aeruginosa* and about 30.8% for *S. aureus*; when the laser power was further increased to 368 mW, the survival rate decreased to 6.4 and 21.1%, respectively.

To investigate the origin of the difference in survival rate from the photothermal effect between the honeycomb substrate and flat substrate, the influence of a temperature rise was examined under infrared laser irradiation with a thermography camera under dry conditions. When using a 10× objective lens, the temperature distribution was confirmed at a laser power of 200 mW (100 mW after transmission through the objective lens): The honeycomb substrate was 94°C, and the flat substrate was 59°C, indicating a more efficient light-heating effect on the honeycomb substrate (fig. S9). By contrast, examination of the temperature distribution at 65 mW (20 mW after transmission through the objective lens) showed that the flat substrate was about 32°C, representing a slight increase from room temperature, whereas the honeycomb substrate was 43°C (fig. S10). These findings indicate that light-induced convection could enable the efficient LIA of bacteria with a high survival rate using HS-LIA.

Theoretical analysis of the photothermal effect

To better understand these phenomena in detail, a theoretical analysis of the photothermal effect and light-induced convection was performed (Fig. 3), assuming the model outlined in fig. S12 (also see Methods). First, the optical response of the gold thin film (50 nm) coated on the surface of the honeycomb substrate used in the experiment was theoretically evaluated by the finite-difference time domain (FDTD) method (fig. S13). Using the obtained values of absorption, temperature distribution, and light-induced convection in a droplet on a substrate, the photothermal effect was theoretically evaluated by simultaneously solving the three equations of mass conservation, momentum conservation, and energy conservation. The results showed that a rotating convection pattern formed in the pores on the surface of the honeycomb substrate in the *xz* cross section (Fig. 3B). As shown in Fig. 3C, it is considered that the bacteria were transported to the observation region, including the laser irradiation point, by horizontal light-induced convection, and collided with the partition walls in the honeycomb pores to become trapped in the region at a millimeter-order distance from the edge of the droplet. Moreover, the temperature was calculated to be about 30°C at a distance of 20 μm from the laser irradiation point, which is sufficiently low for bacterial survival (Fig. 3D). These estimations support the idea that living bacteria could be trapped in a large area and at high density without compromising survival because the honeycomb structure effectively prevents heat conduction.

Application feasibility evaluation

Last, we evaluated the application potential of our proposed system using *Shewanella loihica* as a representative electricity-producing bacterium and assessed the function of the optically assembled bacteria at high density. The honeycomb substrate was used as the working electrode, and a Pt wire was used as the counter electrode. Current measurement was performed while applying a bias voltage of 0.2 V using Ag/AgCl as the reference electrode (Fig. 4; see Methods for experimental details). *S. loihica* is anaerobic and exhibits electron emission by decomposing organic substances using a citric acid circuit. Therefore, the measurement was performed in an environment in which the organic substance (sodium lactate) was decomposed under anaerobic conditions by performing N_2 bubbling to facilitate

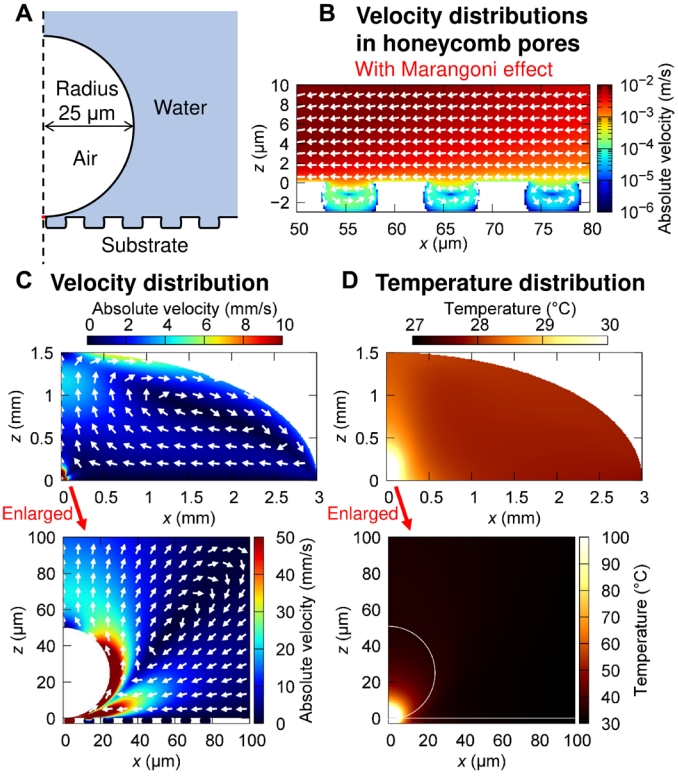

Fig. 3. Simulation of the photothermal effect and light-induced convection. (**A**) Calculation model of light-induced bubble formation and convection. (**B**) Enlarged view of convection in and around the pores on the honeycomb substrate. (**C**) Velocity distribution of light-induced convection. (**D**) Temperature distribution due to the photothermal effect.

electron extraction. For LIA, laser irradiation was performed sequentially for 20 s at each point. In particular, when the number of irradiation points increased to 25, 50, and 100 (Fig. 4A), the current density increased almost proportionally. The current measurement was performed in a short time within 2500 s [in detail, (20 s + 5 s) × 100 points for maximum in the present experiment with 5 s for moving to next point] before cell division. On the other hand, *S. loihica* were trapped by a part of pores in the honeycomb substrate covered with a droplet, where the major part of pores was empty. Therefore, if we would prepare an array of systems with multiple laser beams, we can expect further enhancement of electricity by trapping lots of bacteria over the large area. This result strongly supports the idea that bacteria can be effectively trapped in a live condition with the target function maintained. Moreover, this finding demonstrates the potential of HS-LIA for the development of highly functional microbial devices to best exploit the function of bacteria.

DISCUSSION

A honeycomb substrate coated with a light-absorbing material will be a crucial technology for trapping bacteria in a large area at high density with a high survival rate. Here, we demonstrated the potential of this approach using electricity-producing bacteria as an example of our LIA method with the honeycomb substrate, and improvement of the efficiency of electricity production was confirmed by sequential irradiation of multiple laser beams. Construction of an optical system

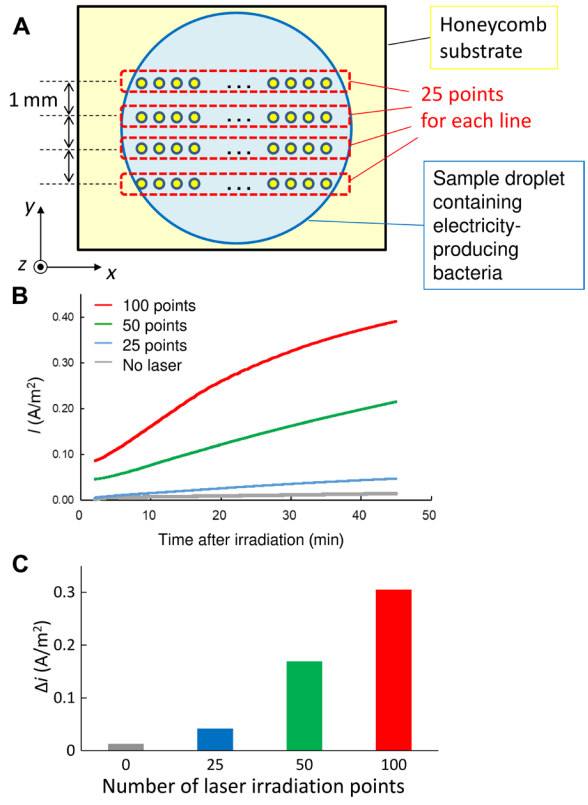

Fig. 4. Current generation by the light-induced accumulation of bacteria. (**A**) Schematic of the experiment of sequential multipoint irradiation. (**B**) Time dependence of the current generated from the electricity-producing bacteria photoinduced and accumulated by multipoint irradiation (the laser irradiation end was set to 0 min). (**C**) Laser irradiation point dependency of the change in current value at the end of laser irradiation. Δ*i*: Difference between the initial current density and final current density.

that can be used for the simultaneous irradiation of multiple laser beams would facilitate the rapid functional evaluation of various types of beneficial microbes. In addition, application of such a system to high-density trapping of other useful microorganisms such as enterobacteria would be expected to achieve innovative progress for the development of a wide variety of microbial-based devices that could resolve long-standing challenges.

METHODS

Production of honeycomb polymer film

Poly(styrene sulfonic acid) sodium salt (64.5 mg) was dissolved in 50 ml of water and stirred well until it became clear (3.17×10^{-3} mol sulfone group is present in a 50-ml solution). Dimethyldioctadecyl ammonium bromide (200 mg) was taken and dissolved in 100 ml of water (there are 3.17×10^{-3} mol ammonium groups in the 200-ml solution). This solution was heated at 70° to 80°C and stirred vigorously until it became translucent. Thereto, 50 ml of a poly(styrene sulfonic acid) sodium salt solution was added and stirred vigorously. Thereafter, the resulting polyion complex particles were separated by suction filtration. Polystyrene (25 mg) and polyion complex (2.5 mg) were dissolved in chloroform (10 ml). This solution was dropped on a cover glass [24 mm (width) by 60 mm (length) by 0.17 mm (thickness); C024601, Matsunami, Japan] and allowed to dry in a humid atmosphere. Three honeycomb polymer membranes were prepared individually, the minor axis diameter and major axis diameter were measured for 50 pores, and the average and SD were obtained. The average major axis diameter of pores was about 5.0 μm, and the average minor axis diameter of them was about 4.6 μm, where the SD for the major and minor axes were less than 0.2 μm. Therefore, the shape of each pore was almost circular. A gold (Au) thin film (thickness, 50 nm) was formed on the surface of the obtained honeycomb polymer film with an ion sputtering apparatus (MC1000, Hitachi, Japan).

Surface observation of honeycomb polymer film

The surface structure of the honeycomb polymer film was observed using a stereomicroscope and a scanning electron microscope. In addition, surface elemental analysis was performed by energy dispersive x-ray analysis. It was also confirmed from energy-dispersive x-ray spectrometry that the main constituent elements of the honeycomb polymer film were carbon and oxygen consisting of polystyrene and contained elements derived from dimethyl distearyl ammonium bromide and sodium polystyrene sulfonate, which were slightly used during preparation (fig. S3A). Au element was also confirmed on the surface of honeycomb polymer film after sputtering (fig. S3B).

Bacteria sample preparation

P. aeruginosa and *S. aureus* were applied to NB agar medium and incubated at optimal temperature for 1 to 2 days. Thereafter, colonies were ingested into the NB liquid medium and then osmotic cultured at an optimum temperature for 18 hours. The concentration of *P. aeruginosa* was measured by Petrifilm Aerobic Count Plate (AC Plate, 3M, USA) and found to be 9.67×10^8 CFU/ml after 48 hours. In addition, the concentration of *S. aureus* was measured by Petrifilm Staph Express Count Plate (STX Plate, 3M, USA) and found to be 1.74×10^8 CFU/ml. The cultured cells were centrifuged (6000 rpm, 5 min), and the supernatant was replaced with deionized distilled water (DDW) and suspended. This operation was repeated twice. Thereafter, fluorescence staining with SYTO 9 and PI was performed using the LIVE/DEAD BacLight Bacterial Viability Kit (L7012, Molecular Probes, USA).

LIA of bacteria

The Au-coated honeycomb substrate was placed on the stage of an inverted microscope (Eclipse Ti-U; Nikon, Japan) with a back port adapter (MMS-2L-800/1064; Sigma Koki, Japan) for laser irradiation (fig. S1). After that, 30 μl of water containing bacteria was dropped on the Au-coated honeycomb substrate. In Fig. 2 and figs. S6 and S7, a laser beam with a wavelength of 1064 nm (10 mW to 70 mW) was irradiated onto the region of droplet on the honeycomb substrate for 20 s through the objective lens [CFI Plan Fluor 100XH(Oil), Nikon, Japan], which is 100× oil immersion objective lens with a numerical aperture of 1.30 and a transmittance of 21.7%. Bacteria were stained with SYTO 9 (480 nm/500 nm) and PI (490 nm/635 nm), and fluorescence images were taken under mercury lamp excitation. Thereafter, the number of trapped bacteria in pores and the survival rate were calculated using the following equations, assuming that the cells stained with SYTO 9 were live bacteria and the bacteria stained with PI were dead: (survival rate) = (number of green luminescent spots − number of red luminescent spots)/(number of green luminescent spots). In fig. S8, similar evaluations were performed with flat Au thin film (10 nm thickness) for the comparison with the previous experiments in (*27*), where the high-power laser was required for the light-induced bubble due to the low efficiency.

Evaluation of photothermal effect of Au-coated honeycomb substrate and flat Au film

The temperature distributions of the Au-coated honeycomb substrate and flat Au thin film were observed by infrared thermal imaging camera (InfReC R550, Nippon Avionics, Japan) with the spatial resolution of 21 μm, as shown in figs. S9 to S11 (we used emissivity = 1 as the default value of InfReC R550). To evaluate the surface temperature with handmade simple optical system, an infrared laser of 975-nm wavelength (PL975P350J-FT900-APC, Thorlabs, USA) near the value of infrared laser for LIA was irradiated onto each substrate through 10× Nikon Plan Fluor Imaging objective lens with a numerical aperture of 0.30 and 16 mm working distance (WD) (N10X-PF, Nikon, Japan).

Electron extraction of electricity-producing bacteria after LIA

2-Hydroxy-1,4-naphthoquinone was added as a mediator to the DM medium to disperse *S. loihica*. Moreover, sodium lactate was also added as an organic substance.

Fifty microliters of the above liquid sample was dropped on the honeycomb substrate and irradiated with a laser. The Au thin film on the upper surface of the honeycomb partition walls was irradiated at 25 points at intervals of about 150 to 200 μm in the x direction (Fig. 4A). Furthermore, photoinduced assembly was performed at 50 points by irradiating two rows in the direction orthogonal to this (y direction) and 100 points by irradiating four rows (row spacing was about 1 mm). The irradiation time at each point was 20 s, and 5 s was required for moving to the next irradiation point after each laser irradiation.

The honeycomb substrate prepared by these procedures was used as the working electrode (diameter of a measured area was 7.5 mm), the Pt wire was used as the counter electrode, and the current was measured under voltage application in a triode system using Ag/AgCl (BAS, RE-1B) as the reference electrode. The measurement was performed under anaerobic conditions with a bias voltage of 0.2 V and N_2 bubbling.

Calculation of light-induced convection in honeycomb-shaped substrate

To solve the temperature and velocity distribution of the incompressive fluid, finite element method simulations were carried out by COMSOL Multiphysics. The governing equations were given by the following steady-state equations of mass, momentum, and energy conservation

$$\nabla \cdot (\rho \mathbf{u}) = 0 \tag{1}$$

$$\rho(\mathbf{u} \cdot \nabla)\mathbf{u} = \nabla \cdot \left[-p\mathbf{I} + \mu\left(\nabla\mathbf{u} + (\nabla\mathbf{u})^{\mathrm{T}}\right) - \frac{2}{3}\mu(\nabla \cdot \mathbf{u})\mathbf{I} \right] + \mathbf{F} \tag{2}$$

$$\rho C_{\mathrm{p}} \mathbf{u} \cdot \nabla T - \nabla \cdot (k \nabla T) = Q \tag{3}$$

where $\mathbf{u}$ is the flow velocity, T is the temperature, ρ is the density, p is the pressure, μ is the dynamic viscosity, C_{p} is the specific heat capacity at constant pressure, k is the thermal conductivity, and Q is the heat source by photothermal effect. $\mathbf{F}$ originates from the buoyancy. The Marangoni effect was also considered. The geometric information of the simulation model is shown in fig. S12, where a cylindrical coordinate system with sixfold rotational symmetry was used. Thermodynamic parameters of the liquid and substrate were considered to be those of water and glass, respectively. The radius of the droplet was assumed to be 3 mm, and the height was 1.5 mm (volume is 28.27 μl, almost the same as that in experiment). As shown in fig. S10B, a bubble (air, diameter: D_{bub} = 0.05 mm) was located above the top of the separation wall of the honeycomb substrate. The laser heating was treated as a point source. Its power was given by AP, where the input power P = 20 mW and the absorption rate of the gold thin film was A = 0.03 evaluated by FDTD in fig. S11. The boundaries except for the symmetric ones were imposed on the heat flux boundary condition assuming the energy loss by $q_0 = h(T_{\mathrm{ext}} - T)$, where the heat transfer coefficient was h = 5 W/m^2 K and the external temperature was T_{ext} = 293.15 K. The slip boundary condition was imposed on the liquid-air interface, and the no-slip boundary condition was imposed on the liquid-solid interfaces. Boussinesq approximation was assumed for water as an incompressible fluid.

SUPPLEMENTARY MATERIALS

Supplementary material for this article is available at http://advances.sciencemag.org/cgi/content/full/6/9/eaaz5757/DC1

Fig. S1. Schematic of experimental setup of LIA of bacteria.
Fig. S2. Preparation and structural evaluation of honeycomb substrate.
Fig. S3. Elemental analysis of honeycomb substrate.
Fig. S4. Behavior of bacteria (*P. aeruginosa*) trapped in pores of honeycomb substrate during laser irradiation under bright-field condition (transparent optical image).
Fig. S5. Survival confirmation of bacteria on honeycomb substrate.
Fig. S6. Fluorescence image of trapped *P. aeruginosa* by changing laser power (20-s irradiation for each).
Fig. S7. Fluorescence image of trapped *S. aureus* by changing laser power (20-s irradiation for each).
Fig. S8. Comparative experiment of LIA of bacteria with flat gold film [thickness: 10 nm in (*27*)].
Fig. S9. Thermographic images of flat Au film and Au-coated honeycomb substrate before and after infrared laser irradiation of 100 mW through 10× dry objective lens (initial power was 200 mW).
Fig. S10. Thermographic images of flat Au film and Au-coated honeycomb substrate before and after infrared laser irradiation of 35 mW through 10× dry objective lens (initial power was 90 mW).
Fig. S11. Thermographic images of flat Au film and Au-coated honeycomb substrate before and after infrared laser irradiation of 20 mW through 10× dry objective lens (initial power was 65 mW).
Fig. S12. Model for the calculation of light-induced convection in honeycomb substrate.
Fig. S13. Simulation of optical response of a gold thin film on the substrate.
Movie S1. An example of fluorescence image of LIA process of *S. aeruginosa* into Au-coated honeycomb substrate (SYTO 9) with a laser power of 40 mW similar to Fig. 2B.
Movie S2. Transparent image of *S. aeruginosa* in Au-coated honeycomb substrate after LIA, which corresponds to fig. S4.

REFERENCES AND NOTES

1. F. M. F. Elshaghabee, W. Bockelmann, D. Meske, M. de Vrese, H.-G. Walte, J. Schrezenmeir, K. J. Heller, Ethanol production by selected intestinal microorganisms and lactic acid bacteria growing under different nutritional conditions. *Front. Microbiol.* **7**, 47 (2016).
2. A. Kumar, L. H.-H. Hsu, P. Kavanagh, F. Barrière, P. N. L. Lens, L. Lapinsonnière, J. H. Lienhard V, U. Schröder, X. Jiang, D. Leech, The ins and outs of microorganism–electrode electron transfer reactions. *Nat. Rev. Chem.* **1**, 0024 (2017).
3. J. L. Round, N. W. Palm, Causal effects of the microbiota on immune-mediated diseases. *Sci. Immunol.* **3**, eaao1603 (2018).
4. P. S. Bonanni, G. D. Schrott, J. P. Busalmen, A long way to the electrode: How do *Geobacter* cells transport their electrons? *Biochem. Soc. Trans.* **40**, 1274–1279 (2012).
5. H. Gong, J. Li, A. Xu, Y. Tang, W. Ji, R. Gao, S. Wang, L. Yu, C. Tian, J. Li, H.-Y. Yen, S. Man Lam, G. Shui, X. Yang, Y. Sun, X. Li, M. Jia, C. Yang, B. Jiang, Z. Lou, C. V. Robinson, L.-L. Wong, L. W. Guddat, F. Sun, Q. Wang, Z. Rao, An electron transfer path connects subunits of a mycobacterial respiratory supercomplex. *Science* **362**, eaat8923 (2018).
6. V. J. Watson, B. E. Logan, Power production in MFCs inoculated with *Shewanella oneidensis* MR-1 or mixed cultures. *Biotechnol. Bioeng.* **105**, 489–498 (2010).
7. X. Chen, D. Cui, X. Wang, X. Wang, W. Li, Porous carbon with defined pore size as anode of microbial fuel cell. *Biosens. Bioelectron.* **69**, 135–141 (2015).
8. C. Zhao, P. Gai, C. Liu, X. Wang, H. Xu, J. Zhang, J.-J. Zhu, Polyanailine networks grown on graphene nanoribbons-coated carbon paper with a synergistic effect for high-performance microbial fuel cells. *J. Mater. Chem. A* **1**, 12587–12594 (2013).
9. G. Widawski, M. Rawiso, B. François, Self-organized honeycomb morphology of star-polymer polystyrene films. *Nature* **369**, 387–389 (1994).

10. O. Karthaus, N. Maruyama, X. Cieren, M. Shimomura, H. Hasegawa, T. Hashimoto, Water-assisted formation of micrometer-size honeycomb patterns of polymers. *Langmuir* **16**, 6071–6076 (2000).
11. P. Escalé, L. Rubatat, L. Billon, M. Save, Recent advances in honeycomb-structured porous polymer films prepared via breath figures. *Eur. Polym. J.* **48**, 1001–1025 (2012).
12. L. Feng, Y. Zhang, J. Xi, Y. Zhu, N. Wang, F. Xia, L. Jiang, Petal effect: A superhydrophobic state with high adhesive force. *Langmuir* **24**, 4114–4119 (2008).
13. F. Xia, L. Jiang, Bio-inspired, smart, multiscale interfacial materials. *Adv. Mater.* **20**, 2842–2858 (2008).
14. A. R. Parker, C. R. Lawrence, Water capture by a desert beetle. *Nature* **414**, 33–34 (2001).
15. M. J. O'Donnell, Site of water vapor absorption in the desert cockroach, Arenivaga investigata. *Proc. Natl. Acad. Sci. U.S.A.* **74**, 1757–1760 (1977).
16. Z. Yin, F. Hannard, F. Barthelat, Impact-resistant nacre-like transparent materials. *Science* **364**, 1260–1263 (2019).
17. D. Ishii, H. Yabu, M. Shimomura, Novel biomimetic surface based on a self-organized metal–polymer hybrid structure. *Chem. Mater.* **21**, 1799–1801 (2009).
18. R. Louise Meyer, X. Zhou, L. Tang, A. Arpanaei, P. Kingshott, F. Besenbacher, Immobilisation of living bacteria for AFM imaging under physiological conditions. *Ultramicroscopy* **110**, 1349–1357 (2010).
19. L. D'Amico, N. J. Ajami, J. A. Adachi, P. R. C. Gascoyne, J. F. Petrosino, Isolation and concentration of bacteria from blood using microfluidic membraneless dialysis and dielectrophoresis. *Lab Chip* **17**, 1340–1348 (2017).
20. H. Okayama, M. Tomita, M. Suzuki, T. Yasukawa, Rapid formation of arrayed cells on an electrode with microwells by a scanning electrode based on positive dielectrophoresis. *Anal. Sci.* **35**, 701–704 (2019).
21. A. Ashkin, J. M. Dziedzic, J. E. Bjorkholm, S. Chu, Observation of a single-beam gradient force optical trap for dielectric particles. *Opt. Lett.* **11**, 288–290 (1986).
22. A. Ashkin, Optical trapping and manipulation of neutral particles using lasers. *Proc. Natl. Acad. Sci. U.S.A.* **94**, 4853–4860 (1997).
23. T. Iida, Control of plasmonic superradiance in metallic nanoparticle assembly by light-induced force and fluctuations. *J. Phys. Chem. Lett.* **3**, 332–336 (2012).
24. Y. Nishimura, K. Nishida, Y. Yamamoto, S. Ito, S. Tokonami, T. Iida, Control of submillimeter phase transition by collective photothermal effect. *J. Phys. Chem. C* **118**, 18799–18804 (2014).
25. M. Ueda, Y. Nishimura, M. Tamura, S. Ito, S. Tononami, T. Iida, Microflow-mediated optical assembly of nanoparticles with femtogram protein via shrinkage of light-induced bubbles. *APL Photonics* **4**, 010802 (2019).
26. T. Iida, Y. Nishimura, M. Tamura, K. Nishida, S. Ito, S. Tokonami, Submillimetre network formation by light-induced hybridization of zeptomole-level DNA. *Sci. Rep.* **6**, 37768 (2016).
27. Y. Yamamoto, E. Shimizu, Y. Nishimura, T. Iida, S. Tokonami, Development of a rapid bacterial counting method based on photothermal assembling. *Opt. Mater. Express* **6**, 1280–1285 (2016).
28. Y. Yamamoto, S. Tokonami, T. Iida, Surfactant-controlled photothermal assembly of nanoparticles and microparticles for rapid concentration measurement of microbes. *ACS Appl. Bio. Mater.* **2**, 1561–1568 (2019).
29. S. Tokonami, T. Iida, Review: Novel sensing strategies for bacterial detection based on active and passive methods driven by external field. *Anal. Chim. Acta* **988**, 1–16 (2017).
30. B. Feng, Z. Li, X. Zhang, Prediction of size effect on thermal conductivity of nanoscale metallic films. *Thin Solid Films* **517**, 2803–2807 (2009).

Acknowledgments: We would like to thank I. Nakase and K. Imura for useful discussions. We also thank Y. Nishimura, R. Ishikura, and K. Hayashi for experimental support. **Funding:** A major part of this work was supported by the JST-Mirai Program (no. JPMJMI18-GA); a Grant-in-Aid for Scientific Research (A) (no. JP17H00856), Grant-in-Aid for Scientific Research (B) (no. JP18H03522), and Grant-in-Aid for Scientific Research on Innovative Areas (no. JP16H06507) from the Japan Society for the Promotion of Science; the Canon Foundation; the Murata Science Foundation; and the Key Project Grant Program of Osaka Prefecture University.
Author contributions: S.T. and T.I. initiated the research and contributed equally to the study design. S.K., R.Y., K.S., T.S., Y.Y., T.I., and S.T. performed the experiments on the LIA of bacteria. S.K., R.Y., K.S., O.K., and S.T. produced the honeycomb substrate. M.T. and T.I. carried out the theoretical calculations. T.I. and S.T. prepared the figures and the manuscript. All authors discussed the results and commented on the manuscript. **Competing interests:** The authors declare that they have no competing interests. **Data and materials availability:** All data needed to evaluate the conclusions in the paper are present in the paper and/or the Supplementary Materials. Additional data related to this paper may be requested from the authors.

Submitted 20 September 2019
Accepted 5 December 2019
Published 28 February 2020
10.1126/sciadv.aaz5757

Citation: S. Tokonami, S. Kurita, R. Yoshikawa, K. Sakurai, T. Suehiro, Y. Yamamoto, M. Tamura, O. Karthaus, T. Iida, Light-induced assembly of living bacteria with honeycomb substrate. *Sci. Adv.* **6**, eaaz5757 (2020).